The Effects of Atmospheric Turbulence on Precision Optical Measurements Used for Antenna-Pointing Compensation

N. Nerheim
Guidance and Control Section

Blind pointing of the Deep Space Network (DSN) 70-meter antennas can be improved if distortions of the antenna structure caused by unpredictable environmental loads can be measured in real-time, and the resulting boresight shifts evaluated and incorporated into the pointing control loops. The measurement configuration of a proposed pointing compensation system includes an optical range sensor that measures distances to selected points on the antenna surface.

This article examines the effect of atmospheric turbulence on the accuracy of optical distance measuremens and describes a method to make in-situ determinations of turbulence-induced measurement errors.

I. Introduction

A method has been investigated [1] to improve the pointing accuracy of the DSN antennas. The method uses optical distance measurements to estimate the shape of the antenna surface and the direction of the associated RF boresight axis. At present, a blind pointing error of about 4–6 millidegrees is achievable. The pointing error increases to about 12 millidegrees under moderately windy conditions. If the full benefits of future plans to increase the operating frequency of the 70-meter antennas to 32 GHz are to be realized, it will be necessary to reduce the blind pointing error to 1-millidegree rms. The goal of the precision optical pointing research is to achieve 1-millidegree pointing accuracy by compensating for wind, thermal, and gravity loadings through the use of precision optical distance measurements.

Analytical study results [1] indicate that 1-millidegree geometric pointing accuracy relative to a stable reference base may be achieved if the distance measurements can be made with an accuracy of about 25–50 μm. The present work examines the effect of atmospheric turbulence on the accuracy of the optical distance measurements and describes a method to make in-situ determinations of turbulence-induced distance errors. The effect of precipitation on optical measurements is discussed briefly.

II. Optical Distance Measurements

The distance measurements will be made with SHAPES (Spatial, High-Accuracy, Position-Encoding Sensor), a JPL-developed time-of-flight range sensor capable of making simultaneous range measurements to multiple targets with submillimeter precision [2].

Optical distance measurements are dependent on the speed of light and therefore on the value of the index of refraction,

n, along the measurement path. If the index does not change with time, an error in the value used for the distance measurement results in a systematic error that has a negligible effect on the pointing accuracy. The presence of turbulence, however, causes random variations in both temporal and spatial values of n that result in random uncertainties in the distance measurements and therefore in the pointing direction.

A. Turbulence and Measurement Errors

The literature concerning the propagation of light through a turbulent atmosphere is extensive. General review articles, of which [3] and [4] are examples, contain long lists of references. Problems associated with turbulence are important for astronomical measurements, laser communication systems, precision optical measurements of distances, and the direction of high-power laser beams. Atmospheric turbulence causes variations of the optical wave amplitude and phase, resulting in beam steering, beam spreading, image blurring, scintillation, and phase fluctuations [5, 6]. Of these effects only phase fluctuations (a 2π-variation of the phase of the optical wave is equivalent to a path-length change of one optical wavelength) affect the accuracy of distance measurements. In [7] and [8] are experimental studies that have a direct bearing on the present work.

Turbulent pressure and humidity fluctuations produce negligible refractive index changes compared to temperature variations; consequently, for optical purposes, "turbulence" refers to atmospheric temperature fluctuations. Nearly all theoretical studies, notably those of Tatarski [9], are based on a model of turbulence proposed by Kolmogorov [10]. The model, which is applicable to both temperature and velocity fluctuations, contains the concept of local isotropy in the fine structure of turbulent flow and justifies the use of statistical methods to study turbulence.

Tatarski's approach to the problem of wave propagation through random media involves the direct solution of a scalar form of the optical wave equation in terms of amplitude and phase fluctuations of the wavefront. Phase variations are formulated in terms of a phase structure function, $D_\phi(\rho)$. For a plane wave of wavelength λ traveling distance L, this structure function is given by

$$D_\phi(\rho) = 2.91 \left(\frac{2\pi}{\lambda}\right)^2 \rho^{5/3} C_n^2 L \qquad \text{(radians)}^2 \qquad (1)$$

where C_n is a measure of the intensity of the turbulence and ρ is the separation of two points on the wavefront normal to the direction of propagation. (For a spherical wave, the constant 2.91 in Eq. (1) is replaced by 1.05.) The phase structure function is related to the more familiar standard deviation of single path phase σ_ϕ, by

$$D_\phi(\rho) = 2\sigma_\phi^2 \, [1 - B(\rho)] \qquad (2)$$

where $B(\rho)$ is the phase autocorrelation function [11].

The 5/3 power dependence on ρ expressed by Eq. (1) is valid out to some maximum value of ρ which is called the "outer scale of turbulence." The outer scale of turbulence, designated here as ρ_m, is roughly equal to the largest eddies in the turbulence. For $\rho > \rho_m$, $B(\rho) = 0$, the rms phase errors of two paths separated by more than ρ_m are not correlated and the relative phase variation between the two paths is just $2\sigma_\phi^2$. This translates into a relative rms path length variation, σ_L, where

$$\sigma_L^2 = \left(\frac{\lambda}{2\pi}\right)^2 2\sigma_\phi^2 = 2.91 \, \rho_m^{5/3} C_n^2 L \qquad \text{m}^2 \qquad (3)$$

The maximum value of $D_\phi(\rho)$ for which Eq. (1) remains valid is not provided by the theory, nor has it been established by experiment. A number of experimental studies of the phase structure function have been made, but none for the condition of very intense turbulence that would cause a problem for the proposed measurements. Consequently, the estimates made below are extrapolated from available experimental data.

The work of Clifford, et al., [8] provides a context for these estimates. The results reported in [8] show excellent agreement with theory (for a spherical wave) up to $D_\phi(\rho) =$ 100 (radians)^2 for ρ = 30 cm on a 70-meter propagation path. Temperature measurements were used to determine the turbulence intensity ($C_n^2 = 10^{-13}$ m$^{-2/3}$) and to determine the outer scale of turbulence. Over a 24-hour period, ρ_m varied between 1 and 2 m with an average of 1.3 m.

The maximum measured value of $D_\phi(\rho)$ reported by Clifford corresponds to an rms distance error of 1 μm. Extrapolating the experimental results to ρ_m = 1.3 m yields $D_\phi(\rho) =$ 1200 radians^2 and σ_L = 3.4 μm.

B. Turbulence-Induced Measurement Errors in SHAPES

SHAPES measures the displacement of selected points on the main reflector relative to a reference point on the sensor optical head. The measurement error includes the intrinsic instrumental error (about 25 μm) and the error due to turbulence. As discussed above, an estimate of the turbulence-induced measurement errors may be obtained from Eq. (3),

provided reliable values of ρ_m and C_n^2 are known. Unfortunately, neither C_n nor ρ_m at the antenna site can be predicted with accuracy. For the present analysis, ρ_m is assumed to be 1.5 m, a value within the range reported in [8], and the value of C_n^2 that would produce a 25-μm distance error (the approximate SHAPES instrumental error) is calculated. If $L = 80$ m is a typical round-trip optical path length and $\rho_m = 1.5$ m, Eq. (3) becomes $\sigma_L^2 = 458\ C_n^2$, and $\sigma_L = 25\ \mu$m requires $C_n^2 = 1.4 \times 10^{-12}\ \mathrm{m}^{-2/3}$.

This value of C_n^2 may be compared with measurements made by a number of workers for various conditions. As an example, a plot [12] of C_n^2 as a function of the time of day is shown in Fig. 1. The measurements were taken on a clear day at a position 2 m above a grassy plain. The figure indicates C_n^2 exceeds $10^{-12}\ \mathrm{m}^{-2/3}$ only for short periods of time when the effects of solar heating are most strongly felt. Insofar as the underlying theory remains valid and the cited conditions resemble those above the antenna, it appears that turbulence will only infrequently degrade the nominal 1-millidegree pointing accuracy.

C. Effect of Precipitation

1. Attentuation by Rain and Fog. The effects of clouds, fog, and rain on electromagnetic wave propagation have been studied extensively [13-17]. Rain (but not fog) strongly attenuates microwaves; consequently, the antennas are situated in rather dry climates [14]. Both fog and rain are known to attenuate optical radiation.

The effect of fog at visible wavelengths is generally reported as visibility, which is defined in terms of attenuation [18]. For example, if the visibility is 0.25 miles, an optical signal would be reduced by 3.4 dB over an 80-m path. Attenuation of optical signals degrades the SHAPES measurement accuracy; part of the instrumental error is inversely proportional to the square root of the received signal energy. A 3.4-dB loss of signal would increase the instrument error from a nominal value of 25 μm to about 32 μm.

The effects of rain on the propagation of optical radiation have been measured at a number of wavelengths. It has been shown [15] that the attenuation, α, in heavy rain may be expressed as $\alpha = 0.155\ r + 2.66$ dB/km where r is the rate of rainfall in mm/hr. At a rate of 15 mm/hr, which is considered moderate to heavy rainfall, the optical attenuation over an 80-m path is about 0.4 dB, a value that would increase the SHAPES measurement error by only about 2 percent. The impact of such rainfall on microwave antenna performance would be much more severe [14], leading to the observation that rain is a more serious problem for antenna operation than for SHAPES measurements.

2. Average Rain and Fog at Goldstone and Their Impact on SHAPES Operation. Climatological data for airfields have been published by the U.S. Navy [19]. The data for fog applicable to the present problem are expressed as a percentage of weather observations for which visibility was less than one mile for any period of time during 3-hour observation periods. At Daggett, California, (about forty miles south of and climatologically similar to the JPL antenna site at Goldstone), visibility less than one mile was reported for 0.5 percent of the observations.

The annual rainfall at Daggett [19] is 3.6 inches. Studies have shown that the duration of any rainfall rate (e.g., 15 mm/hr) is well-correlated with the total annual rainfall [14]. Based on this correlation, the rate at Goldstone should not exceed 15 mm/hr for more than about 15 minutes per year. One concludes that because of the dry climate at Goldstone, the effects of rain and fog on SHAPES operation are negligible.

III. SHAPES Measurements of Turbulence-Induced Path Length Variations

The following describes a method by which SHAPES can be used to determine the rms magnitude of turbulence-induced variations in optical path length. The method relies on the form of SHAPES measurement errors and the use of two coincident but separable optical paths to isolate turbulence-induced variations.

A. SHAPES Measurement Errors

SHAPES range measurements are based on the time required for a laser pulse to travel the round-trip distance from source to detector, usually via an intermediate retroreflector target. The laser is pulsed at frequency f and the pulses are separated by an effective wavelength λ, given by

$$\lambda = \frac{c}{nf} \tag{4}$$

where c is the speed of light and n is the refractive index at the optical wavelength (0.78 μm) of the laser pulse along the optical path.

The target range relative to a reference position may be written as

$$R = N\frac{\lambda}{2} + \Delta R = \frac{Nc}{2nf} + \Delta R \tag{5}$$

where N is the integer number of wavelengths in the optical path and ΔR is the SHAPES measurement. N may be calcu-

lated exactly from the known geometry of the antenna measurements.

Measurement errors consist of the SHAPES instrument error and errors in λ. Variation of the SHAPES operating frequency is negligible; hence, from Eq. (4), only errors in the atmospheric refractive index contribute to the error in λ and $\sigma_\lambda \simeq \lambda\sigma_n$ for $n \simeq 1.0$.

Standard error analysis applied to Eq. (5) now yields

$$\sigma_R^2 = \left(\frac{N}{2}\right)^2 \sigma_\lambda^2 + \sigma_{\Delta R}^2 \tag{6}$$

or

$$\sigma_R^2 = R^2 \sigma_n^2 + \sigma_{\Delta R}^2 \tag{7}$$

where $\sigma_{\Delta R}$ is the SHAPES instrument error, and $R^2\sigma_n^2$ is the portion of the range variance that is due to the random fluctuations of n as given by σ_L of Eq. (3).

B. Evaluation of Turbulence Effects with SHAPES

As noted above, SHAPES range measurements typically involve laser pulses that travel a round trip from a pulsed laser mounted very near the sensor head to a retroreflector and back to the sensor head. However, the tip of an optical fiber may be co-located with the retroreflector and used to direct a train of laser pulses at SHAPES; the optical path length through the air for these pulses is half that for the retroreflected pulses. Measurements of turbulence-induced range error may then be obtained by comparing the standard deviations of simultaneous measurements made over the fiber and retroreflected paths. The pulse propagation time through the fiber will vary with temperature but this verification has a long time constant and is unaffected by turbulence during the measurement period.

For the fiber-originated path, Eq. (7) becomes

$$\sigma_R^2 = \left(\frac{R}{2}\right)^2 \sigma_n^2 + \sigma_{\Delta R}^2 \tag{8}$$

Because the instrument error is identical for the two simultaneous measurements of the same signal strength, the difference of Eqs. (7) and (8) is

$$\sigma_2^2 - \sigma_1^2 = 0.75\, R^2 \sigma_n^2 \tag{9}$$

where the subscripts 2 and 1 refer to the double and single paths respectively. Equation (9) indicates that SHAPES can be used to measure the effects of turbulence on antenna distance measurements provided these effects are sufficiently large compared to the sensor's intrinsic resolution.

IV. Laboratory Demonstration of Turbulence Measurements Using SHAPES

A. Experimental Procedure

The sensitivity of SHAPES to turbulence-induced errors in range measurements has been demonstrated in laboratory experiments. No attempt was made to reproduce the open air turbulence of the antenna site: the measurements merely demonstrate the capability of SHAPES to detect and measure errors due to turbulence.

A sketch of the experimental setup is shown in Fig. 2. Two retroreflector targets, T_r and T_a, located about 10 m from the sensor, were illuminated by laser L_a. A second target, T_b, also located at a distance of 10 m, was illuminated by a second laser, L_b. Turbulence was generated in the optical path between the sensor and target T_b by an electrical heater.

The return from each target ultimately forms an image on the SHAPES CCD. The relative position of the image's centroid, x, is directly related to the target's range. The reference centroid, x_r, is subtracted from each of the other target centroids x_i, to form the quantity $y_i = x_i - x_r$. The standard deviation of each y_i, σ_{yi}, was calculated from 94 consecutive measurements.

The targets T_a and T_r are located at the same range and are illuminated by a single laser; the measurement error σ_{ya} thus consists of only the CCD readout errors, $\sigma_{x_a} = \sigma_{x_r} = \sigma_x$, of the two centroids,

$$\sigma_{ya}^2 = \sigma_{x_a}^2 + \sigma_{x_r}^2 = 2\sigma_x^2 \tag{10}$$

Because targets T_b and T_r are illuminated by separate lasers, determination of y_b is subject to an additional error, σ_ϕ, associated with jitter in the relative firing times of the two lasers. Thus, in the absence of turbulence,

$$\sigma_{yb}^2 = 2\sigma_x^2 + A^2 \sigma_\phi^2 \tag{11}$$

where A is a constant proportional to the streak tube drive voltage.

Detection of turbulence depends on the increase in σ_{yb} caused by the turbulence. If the turbulence-induced error is designated by σ_t, the variance of y_b becomes

$$\sigma_{y2}^2 = 2\sigma_x^2 + A^2 \sigma_\phi^2 + \sigma_t^2 \tag{12}$$

The difference of Eqs. (12) and (11) gives the desired turbulence-induced error.

Laboratory measurements were made with and without the heater-generated turbulence, and the difference in the calculated variance with and without turbulence was assigned to σ_t^2. Measurements of σ_{ya}^2 verified that the turbulence did not affect the optical path of L_a.

The laboratory experiments used to determine σ_t require that both σ_x and σ_ϕ remain constant for all measurements. The method proposed for determining $R\,\sigma_n$ above the DSN antennas eliminates this requirement by performing simultaneous measurements of single- and double-path values of σ_y.

B. Results and Discussion

The results of one set of experiments are shown in Table 1. The relationship between range and CCD centroid position depends on the amplitude of the streak tube drive voltage: for this experiment, $\sigma_{\Delta R} = 800\ \sigma_y\ \mu$m and thus

$$R\,\sigma_n = 800\ \sigma_t\ \mu\text{m} = \sqrt{\sigma_{\Delta R}^2 - (12\ \mu\text{m})^2}$$

where 12 μm is the average value of $\sigma_{\Delta R}$ with no turbulence.

The results shown in Table 1 vary with heater power and heater location. Increasing heater power, which was expected to increase the turbulence intensity, caused an increase in the measurement error. Moving the heater to increase the turbulence path length also produced increased measurement error. The use of a constant value of 12 μm for the instrument error is validated by the nearly constant value of $\sigma_{\Delta R}$ (10–13 μm) when the heater was turned off.

The results of the laboratory experiments demonstrate that SHAPES measurements may be used to sense atmospheric turbulence. Although natural turbulence at the antenna site is expected to be very different from that produced in the laboratory, the laboratory experiments suggest that SHAPES may be used to make in-situ measurements of turbulence on the antenna. The results also show that, in the presence of sufficient turbulence intensity, optical range measurements may be in error by an amount that is significant for the proposed compensation scheme.

V. Conclusions

A proposed method to achieve 1-millidegree geometric pointing accuracy of the DSN 70-meter antennas makes use of multi-point optical measurements of high precision. Heavy rain and intense fog degrade optical measurements. However, because of the dry climate at most antenna sites, these events occur infrequently and their effect on antenna operation is negligible. Atmospheric turbulence produces errors in the optical measurements that degrade the derived pointing precision. The results of the present study suggest that turbulence will not seriously degrade the pointing precision except for very limited periods of intense turbulence caused by solar heating of the air above the antenna. The precision pointing system [1] requires knowledge of the measurement error to evaluate the pointing error. During operational periods, the variance of the SHAPES measurements, turbulence-related and otherwise, can be determined and the degradation of the pointing accuracy assessed. Additional measurements allow the part of the error caused by turbulence to be determined.

References

[1] R. Scheid, "Precision Pointing Compensation for DSN Antennas with Optical Distance Measuring Sensors," *TDA Progress Report 42-97*, vol. April–June 1989, Jet Propulsion Laboratory, Pasadena, California, this issue.

[2] J. McLauchlan, W. Goss, and E. Tubbs, "SHAPES: A Spatial High-Accuracy, Position-Encoding Sensor for Space-Systems Control Applications," in *Proceedings of the Annual Rocky Mountain Guidance and Control Conference*, January 30–February 3, 1982, Keystone, Colorado, pp. 371-382, 1982.

[3] R. S. Lawrence and J. W. Strohbehn, "A Survey of Clear-Air Propagation Effects Relevant to Optical Communications," *Proc. IEEE*, vol. 58, no. 10, pp. 1523-1545, 1970.

[4] A. Ishimaru, "Theory of Optical Propagation in the Atmosphere," *Opt. Eng.*, vol. 20, no. 1, pp. 63-70, 1981.

[5] J. I. Davis, "Considerations of Atmospheric Turbulence in Laser Systems Design," *Appl. Opt.*, vol. 5, pp. 139-147, 1966.

[6] K. S. Shaik, "Atmospheric Propagation Effects Relevant to Optical Communications," *TDA Progress Report 42-94*, vol. April-June 1988, Jet Propulsion Laboratory, Pasadena, California, pp. 180-200, August 15, 1988.

[7] G. N. Gibson, J. Heymay, J. Lugten, W. Fitelson, and C. H. Townes, "Optical Path Lengths in Atmosphere," *Appl. Opt.*, vol. 14, pp. 4383-4389, 1984.

[8] S. F. Clifford, G. M. B. Bouricius, G. Ochs, and M. H. Ackley, "Phase Variations in Atmospheric Propagation," *J. Opt. Soc. Am.*, vol. 61, pp. 1279-1284, 1971.

[9] V. I. Tatarskii, *Wave Propagation in a Turbulent Medium*, New York: McGraw-Hill, 1961.

[10] A. N. Kolmogorov, "The Local Structure of Turbulence in Incompressible Viscous Fluid for Very Large Reynolds Numbers," *Soviet Physics Uspekhi*, vol. 10, no. 6, pp. 734-736, May-June 1968.

[11] R. E. Hufnagel, "Variations of Atmospheric Turbulence," in *The Infrared Handbook*, Chapter 6, USGPO, Washington, D.C., 1974.

[12] R. S. Lawrence, G. R. Ochs, and S. F. Clifford, "Measurements of Atmospheric Turbulence Relevant to Optical Propagation," *J. Opt. Soc. Am.*, vol. 60, pp. 826-830, 1970.

[13] D. C. Hogg and T. S. Chu, "The Role of Rain in Satellite Communications," *IEEE Proc.*, vol. 63, pp. 1308-1331, 1975.

[14] P. D. Potter, M. S. Shumante, C. T. Stelzried, and W. H. Wells, "A Study of Weather-Dependent Data Links to Deep Space Applications," *JPL Technical Report 32-1392*, Jet Propulsion Laboratory, Pasadena, California, 1969.

[15] T. S. Chu and D. C. Hogg, "Effects of Precipitation and Propagation at 0.63, 0.35 and 10.6 Microns," *Bell System Tech. J.*, vol. 47, pp. 723-759, 1960.

[16] G. C. Mooradian, M. Geller, L. B. Stotts, D. H. Stevenson, and R. A. Krautwald, "Blue-Green Pulsed Propagation Through Fog," *Appl. Opt.*, vol. 18, pp. 429-441, 1979.

[17] G. C. Mooradian, M. Geller, P. H. Levine, L. B. Stotts, and D. H. Stevenson, "Over the Horizon Optical Propagation in a Maritime Environment," *Appl. Opt.*, vol. 19, pp. 11-30, 1980.

[18] R. G. Fleagle and J. A. Businger, *An Introduction to Atmospheric Physics*, Orlando, Florida: Academic Press, Inc., 1980.

[19] U. S. Naval Weather Services, *World-Wide Airfield Summaries*, Vol. VIII, Part I, Asheville, North Carolina, 1969.

Table 1. Effect of turbulence on SHAPES measurement error

Test No.	Description	$\sigma_{\Delta R}$, μm	$R\sigma_n$, μm
1	Turbulence	19	14
2	No turbulence	10	–
3	Turbulence (repeat no. 1)	19	14
4	Turbulence (increase heater power)	26	23
5	Turbulence (move heater to increase turbulence)	38	35
6	No turbulence	13	–
7	Turbulence (reduce power)	22	18
8	No turbulence	12	–

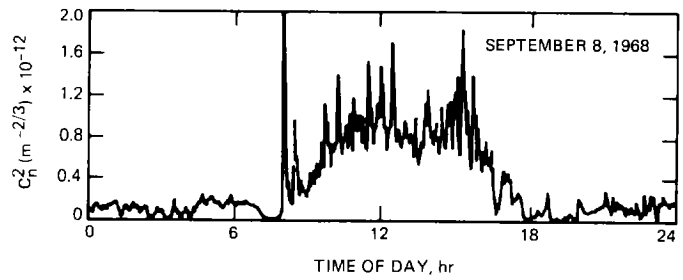

Fig. 1. Refractive index structure parameter versus time of day. The measurements were derived from temperature measurements made on a clear day at an elevation of 2 m above a grassy plain [11].

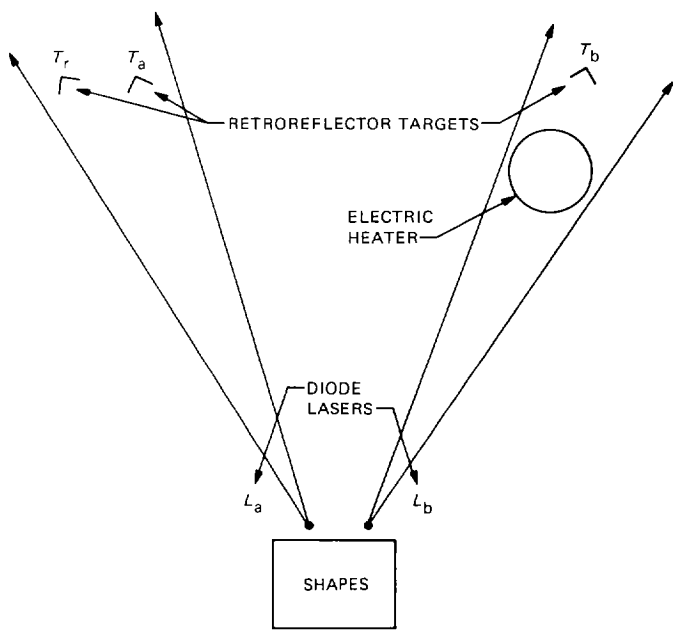

Fig. 2. Sketch of a laboratory experiment to demonstrate the sensitivity of SHAPES to turbulence-induced range errors.